Extended Abstracts of the 2012 International Conference on Solid State Devices and Materials, Kyoto, 2012, pp981-982

Novel High-sensitivity Broadband Image Sensor with CIGS Thin Films

Yuji Ota[1], Takuji Maekawa[1], Osamu Matsushima[1], Hiroshi Sekiguchi[1], Toshihisa Maeda[1], Tetsuo Fujii[1], Dai Ohnishi[1], Hidemi Takasu[1] and Shigeru Niki[2]

[1] Photonics Research and Development Headquarters, Rohm Co., Ltd.
21 Mizosaki-cho Saiin, Kyoto 615-8585, Japan
Phone: +81-75-321-1465 E-mail: Yuji.Ota@dsn.rohm.co.jp
[2] National Institute of Advanced Industrial Science & Technology
Tsukuba Central 4, Higashi 1-1-1, Tsukuba, Ibaraki, 305-8562, Japan

1. Introduction

Polycrystalline chalcopyrite semiconductors have been widely developed as absorber materials of thin film solar cells. One of the materials is $Cu(In,Ga)Se_2$ (CIGS), the absorption coefficient of which is two orders of magnitude higher than that of Si. Moreover, CIGS has a direct bandgap, which can be tuned from 1.0 to 1.7 eV by varying the ratio of the number of Ga atoms to group-III atoms (Ga/III ratio). CISG based thin film solar cells already have been commercialized taking advantage of not only the high absorption coefficient but also the long-term durability [1-3].

We have applied a polycrystalline CIGS thin film to image sensors based on complementary metal-oxide semiconductor (CMOS) technology. The use of CIGS as a light receiving part can add high sensitive and broadband characteristics to conventional Si-based CMOS image sensors. Figure 1 shows a typical appearance of the CIGS-based image sensor developed in this work. The image sensor is based on 656 × 488 pixels with 7.5 μm × 7.5 μm pixel sizes (Table I). Unlike in the case of solar cells, leakage current density must be decreased by several orders of magnitude in order to obtain images with minimum fixed pattern noise (FPN). The pixel isolation technique was conducted by using dry and wet etching technique [4,5]. As a result, the leakage current density was about 10^{-8} A/cm^2, the value of which still needs to be reduced by one order of magnitude toward a practical application.

Table I Specifications of CIGS sensor

Photoelectric surface	CIGS
Pixel Size	7.5 μm × 7.5 μm
Total Pixels	712(H) × 512(V)
Effective Pixels	656(H) × 488(V)
Spectral Responsivity	400-1200 nm

In this work, CIGS-based image sensors have been fabricated without pixel isolation technique, which could bring about a trade-off relationship between the leakage current and the electric crosstalk effect. The optimization of the image sensor structure will be discussed and the application of the CIGS-based image sensor will be introduced.

2. Experimental Procedure

A new schematic structure of the image sensor, which consists of n-ZnO:Al/i-ZnO/CdS/CIGS/W/CMOS circuit is shown in Fig. 2. Firstly, W backside electrodes are fabricated on CMOS circuit by chemical vapor deposition. Although Mo is widely used as a backside electrode in CIGS solar cells, W matches up with a silicon process. We have replaced Mo with W as a backside electrode [6] and have confirmed that the quantum efficiency and leakage current of the CIGS-based image sensor do not change between W and Mo electrodes. A p-type CIGS layer of 0.6–1.6 μm is deposited on the W electrode formed CMOS wafer by using a three-step co-evaporation method, in which the Ga/III ratio are adjusted to the values between 0.3 and 0.5. The CIGS deposition temperature is set at below 450°C, which is slightly lower than conventional CIGS deposition temperature for solar cells, for the purpose of providing protection against thermal damages on Al in CMOS circuits. Next, a buffer layer of CdS is formed by chemical bath deposition method followed by double window layer of undoped and Al doped ZnO deposition by sputtering. Finally, the device is completed by forming an Al/TiN grid as the top electrode. Shown in Fig. 3 is a cross-section scanning electron microscope (SEM) image of the CIGS-based image sensor.

3. Results and discussion

The pixel isolation technique has a limitation to decrease the dark current less than 10^{-8} A/cm^2 due to the etching damage. Although the continuous CIGS layer causes the electric crosstalk effect, controlling electrical field in the CIGS layer permits taking a crisp image with a low dark current of about 10^{-9} A/cm^2. A resolution chart image obtained with the CIGS-based image sensor is presented in Fig. 4.

Figure 5 shows the quantum efficiency spectra obtained from the devices with different CIGS thicknesses. The quantum efficiency at near infrared (NIR) region increases with increasing CIGS thickness. It is found that the CIGS layer with the thickness less than 1 μm is not sufficient for absorbing NIR light. In order to apply the CIGS-based image sensor to NIR regions, the CIGS thickness of 1.2 μm or more is required to convert most part of photons in NIR

region into carriers.

Shown in Fig. 6 is a hand image captured by CIGS-based image sensor under NIR light irradiation. The NIR light passes through human skin and is absorbed in the hemoglobin in blood vessels. The CIGS-based image sensor, which has a higher sensitivity in the NIR light than a image sensor with Si, can make them distinct.

4. Conclusions

The combination of LSI and solar cell technologies has realized the image sensor that outperforms conventional Si-based CMOS image sensors. The optimization of the sensor structure has enhanced the characteristics of NIR imaging. The new image sensor is expected to be widely applied for automotive and security cameras designed to operate in a wide range of lighting conditions, from glaringly bright to extremely dim, as well as in biometric technologies for iris and vein authentication.

References

[1] A. M. Gabor, J. R. Tuttle, D. S. Albin, M. A. Contreras and R. Noufi, *Appl. Phys. Lett.* **65** (1994) 198-200.

[2] N. Kohara, T. Negami, M. Nishitani and T. Wada , *Jpn. J. Appl. Phys.* **34** (1995) 1141-1144.

[3] K. Sakurai, R. Hunger, R. Scheer, C. A. Kaufmann, A. Yamada, T. Baba, Y. Kimura, K. Matsubara, P. Fons, H. Nakanishi, S. Niki, *Prog. Photovolt. Res. Appl.*, **12** (2004) 2.

[4] O. Matsushima, K. Miyazaki, M. Takaoka, T. Maekawa, H. Sekiguchi, T. Fuchikami, M. Moriwake, H. Takasu, S. Ishizuka, K. Sakurai, A. Yamada and S. Niki, *IEDM* **1109** (2008) 10.

[5] K. Miyazaki, O. Matushima, M. Moriwake, H. Takasu, S. Ishizuka, K. Sakurai, A. Yamada and S. Niki, *Thin Solid Films* **517** (2008) 7.

[6] K. Orgassa, H. W. Schock, *Thin Solid Films* **431** (2003) 387.

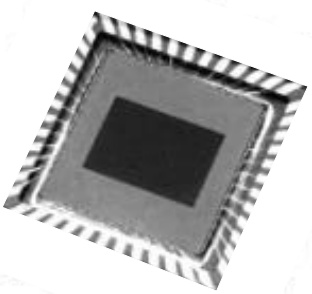

Fig. 1 Chip photograph. The completed sensor is packaged in a standard 48-pin package

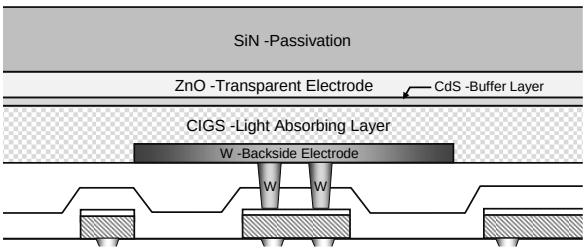

Fig. 2 Schematic structure of CIGS-based image sensor

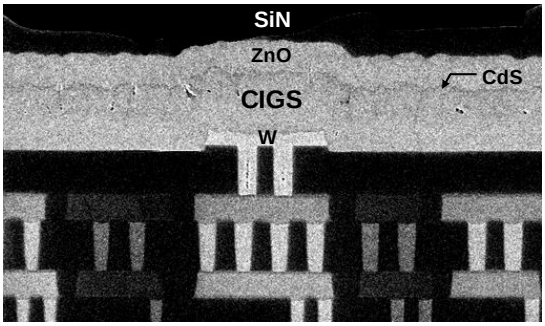

Fig. 3 SEM cross-section of CIGS-based image sensor

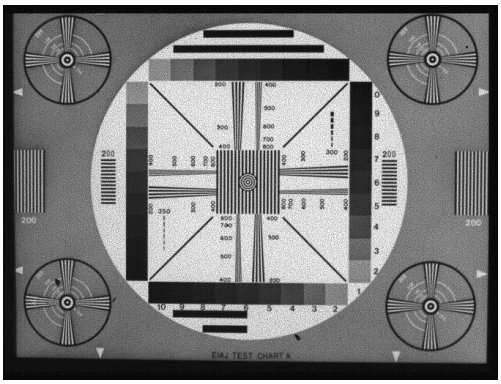

Fig. 4 Resolution chart image captured with CIGS-based image sensor

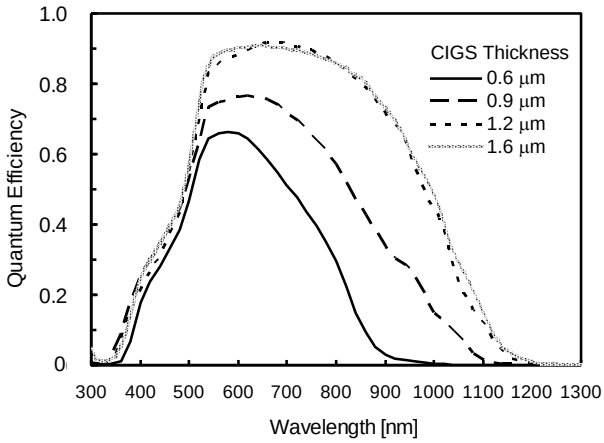

Fig. 5 Quantum efficiency as a function of the CIGS thickness.

Fig. 6 Hand image captured by CIGS-based image sensor under NIR light irradiation.